Int J Adv Manuf Technol (2016) 85:443–454
DOI 10.1007/s00170-015-7944-y

ORIGINAL ARTICLE

Optimization of pre-polishing parameters on a 5-axis milling machine

Mourad Moumen[1] · **Julien Chaves-Jacob**[2] · **Mohamed Bouaziz**[1] · **Jean-Marc Linares**[2]

Received: 28 May 2015 / Accepted: 4 October 2015 / Published online: 15 October 2015

Abstract Pre-polishing and polishing stages are considered as semi-finishing and finishing operations in manufacturing process. Generally, these operations are carried out manually. These stages are health hazards for the operator and may lead to geometrical defects during manufacturing. This paper proposes and optimizes a method to perform these operations on a common 5-axis milling machine. This method uses the flank of a flexible cylindrical tool to link the machine position and the exerted polishing pressure. The toolpath proposed comprises a carrier trajectory on which a loop pattern is repeated. Subsequently, experimental optimization of the pre-polishing cost is proposed, coupled with an estimation of the roughness obtained. Firstly, a screening design of experiments is used to identify the most influential factors of this process. Based on these influential factors, a response surface is used to obtain experimental models to estimate the pre-polishing cost per volume and resulting roughness. These models are used to optimize the pre-polishing factors to reduce the process cost while maintaining specific roughness.

Keywords Toolpath · 5-axis milling · Polishing · Biomedical · Optimization

Electronic supplementary material The online version of this article (doi:10.1007/s00170-015-7944-y) contains supplementary material, which is available to authorized users.

✉ Julien Chaves-Jacob
julien.chaves-jacob@univ-amu.fr

[1] Ecole Nationale Polytechnique, Département de Génie Mécanique, Laboratoire de Recherche Génie Mécanique et Développement, 10 Avenue, Hassan Badi, BP 182, El-Harrach, Algiers 16200, Algeria

[2] Aix-Marseille University, CNRS, ISM UMR 7287, 13288, Marseille Cedex 09, France

1 Introduction

Nowadays, pre-polishing and polishing operations are carried out manually. For example, Hilerio et al. [1] present the product life management (PLM) of knee prostheses. Figure 1 shows the production process of a femoral part of a knee prosthesis and highlights manual pre-polishing and polishing operations. These operations are health hazards for the operator. These polishing stages imply repetitive and controlled movements (damaging for human joints) and generate small airborne particles. A study presented by Lison et al. [2] emphasizes the pathogenesis of lung disease produced by airborne cobalt particles (standard alloy used for these prostheses). Furthermore, the geometrical result of the polishing steps, performed manually, depends on the operator's skills and experience.

Pre-polishing operations are intended for reducing surface roughness (generated through milling, casting, etc.) and for reducing the polishing step time. To carry out this stage, a machine able to do complex kinematics and access all sides of the free-form surfaces must be used. Another fundamental issue, when carrying out pre-polishing operations with a computer numerical control (CNC) machine, is to control the contact force between the polishing tool and the workpiece. In fact, an operator can adapt the pre-polishing toolpath to exert a constant force between the tool and workpiece while a machine is commonly controlled only in position.

In recent years, the scientific community has tried to specify a process to automate free-form surface polishing. To do this, authors have proposed to develop specific machines. Tsai and Huang [3] designed a specific 5-axis machine to carry out polishing operations. A force control loop was developed on this machine. The polishing operation was carried out with a flexible foam-laminate tool on which sandpaper was mounted. Roswell et al. [4] proposed a specific machine using the

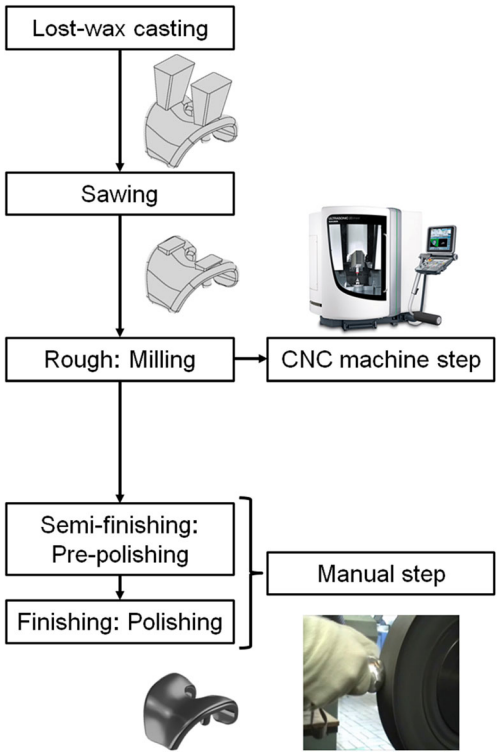

Fig. 1 Production of knee prostheses

pneumatic control of polishing forces through pressure control; this machine is also used in the research of Liao et al. [5]. The proposed machine comprised two linear crossed axes on which a robot tripod was mounted. This solution used a rigid grinding tool. To estimate the induced polishing pressure, authors used a hertz model. Moreover, 5- and 6-axis industrial robots may be used to carry out pre-polishing and polishing operations. This type of robots is interesting due to its low cost, but in return, its position accuracy is reduced due to its low rigidity (about 0.1 mm). Ryuh et al. [6] have used a 6-axis robot on which a pneumatic system was adapted to control the applied polishing force. Nagata et al. [7] added a combined control of the tool position and force on a 6-axis robot to polish free-form molds. Lin and Lu [8] proposed to carry out free-form surface polishing with a 6-axis robot. They adapted and smoothed a milling toolpath generated by a standard CAM system.

Frequently, pre-polishing and polishing stages are carried out after a milling operation. Thus, authors used the milling machine directly to conduct such finishing stages. The method has the advantage of preventing the loss of the workpiece reference frame. Wu et al. [9] suggested that a 3-axis milling machine can be used to polish free-form surfaces with flexible ball-end milling. Polishing with a 3-axis machine requires the use of a ball-end tool to solve this problem, and authors recommended the use of a 5-axis milling machine. Pessoles and Tournier [10] used a 5-axis milling machine on which a flexible disk, with sandpaper attached to the end, was mounted. An experimental study was carried out to estimate the stiffness of the tool. This stiffness is used to estimate the polishing force generated by tool deformation. Thus, the flexible tool is used to obtain a smooth connection between the CNC position and the applied force. Feng et al. [11] used a similar process and proposed a theoretical study to predict the force exerted. Chaves-Jacob et al. [12] used the flank of a flexible cylinder tool to carry out polishing operations on a 5-axis milling machine.

To optimize the pre-polishing and polishing stages, the material removal flow rate needs to be estimated. It is difficult to estimate the material removal flow rate which depends on a wide range of parameters. Thus, Tsai and Huang [3] used an empirical approach with design of experiments (DOE) to optimize polishing parameters. Wang et al. [13], using a numerical model, demonstrated that the material removal flow rate is mainly influenced by polishing contact pressure. At the same time, roughness and undulation must be controlled. The flexibility or inflexibility of the tool will greatly influence the polishing roughness obtained. Numerous authors studied rigid tools, similar to grinding operations. Ahn et al. [14] proposed an experimental approach based on an acoustic recording of the polishing process to estimate roughness obtained. Using this information, Ahn et al. [14] optimized polishing pressure, feed rate, and tool wear. Denkena et al. [15] theoretically estimated the roughness with a rigid corner-radius end tool used in a 5-axis machine. This model was made based on the nominal tool envelope. This model estimates the surface obtained, and it was used to derive roughness indicators. Savio et al. [16] suggested another approach based on the Abbott–Firestone curve. Hertz theory was used to determine the tool engagement to clip the Abbott–Firestone curve at a defined height. The last two models consider only the tool envelope. Xi and Zhou [17] proposed a method to estimate surface roughness, considering the tool as a set of grits (defined by its position and diameter). This method was started out by modeling the polishing tool. In this study, the value of grit diameter is randomly selected. Thereafter, the tool obtained was used to perform virtual geometrical machining of the workpiece material. Furthermore, roughness estimations, using a flexible tool, are commonly carried out experimentally as presented by Huissoon et al. [18].

This paper proposes and optimizes a process to carry out the pre-polishing stage on a 5-axis CNC milling machine. The first section will present the pre-polishing method and associated parameters. These parameters are classified into two categories: process parameters and toolpath parameters. The second section will propose a screening design of experiment to indentify the main factors influencing pre-polishing cost. The last section will develop proposed pre-polishing process optimization. This optimization was undertaken to reduce the production cost while maintaining acceptable roughness.

2 Pre-polishing process on a 5-axis CNC machine

The proposed method uses the cylindrical flank side of a polishing tool. Presented developments are carried out with pre-polishing on free-form surfaces. To perform this operation, a 5-axis CNC machine is used. The use of the tool flank to pre-polish a free-form surface imposes the tool axis variation along the toolpath, hence the use of a 5-axis machine. The method is illustrated in Fig. 2. The toolpath used comprises carrier trajectories which cover the whole polished surface. The elementary patterns are added on these carrier toolpaths to obtain a looping movement. Figure 3 presents an example of a polished pattern on an industrial workpiece. One of the aims of this paper is to optimize this elementary pattern shape. On the other hand, the use of a CNC machine tool induces the problem of controlling the pressure contact between the tool and the polished surface. A CNC machine controls the tool position in relation to the polished surface. However, one of the main parameters in a polishing operation is the tool contact pressure on the surface. Thereby, a flexible tool is used to carry out the polishing operations on a CNC machine. The elasticity of the tool is used to link the polishing pressure to the tool position. The determination of the radial stiffness of the flexible tool is performed experimentally using a force sensor. The control of this radial force is developed by Chaves-Jacob et al. [19]. The proposed method is defined by parameters linked to the process and the toolpath.

2.1 Pre-polishing process parameters

The pre-polishing process presented is carried out with a flexible tool. This tool is composed of a rubber support on which an abrasive cap is mounted. Active part of the tool is sandpaper caps composed of corundum applied on a woven support and fixed by a resins bond. Different caps are available with different grit sizes. The grit size is defined by a number; when this number increases, the grit size decreases. For example, caps with grit numbers of 150 and 320 have an average grit size of 100 and 46 μm, respectively.

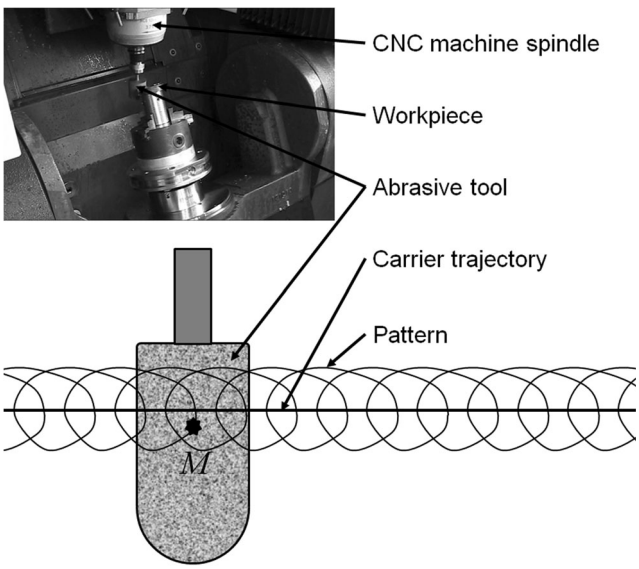

Fig. 2 Illustration of the polishing method

Furthermore, the polishing process has intrinsic characteristics such as the following kinematic parameters: spindle rotation speed (*RPM*) and feed rate (V_f) expressed in rotations per minute and millimeters per minute, respectively. During pre-polishing, lubrication may be added to improve the polishing operation. Radial engagement is also one of the process parameters, but this parameter has a specific role in polishing. A nominal radial engagement is specified during the process. This nominal engagement induces tool deformation which creates the tool contact pressure. The material removal rate is directly linked to the contact pressure. If the contact pressure returns to zero, the material removal also returns to zero. The toolpath also comprises an important role as regards the pre-polishing process. Section 2.2 hereinafter details all the toolpath parameters.

2.2 Toolpath parameters

The toolpath plays an important role as regards the pre-polishing process. The toolpath proposed is composed of a carried toolpath used to cover the entire surface and an elementary pattern repeated along this carried toolpath. The morphology of this pattern directly determines the number of times that the tool will pass on an elementary workpiece surface.

The elementary pattern is based on the trochoidal curve. Figure 4a illustrates the trochoidal pattern and its two main parameters. The first parameter, R, defines the amplitude of the trochoidal pattern. Parameter a defines the progression by looping. The pattern shape is defined by the previous two parameters. Three pattern morphologies exist:

- $a<<R$: the pattern resembles a circle. This type of pattern passes many times over a same point on the surface.
- $a=R$: the pattern passes exactly 3 times over each point on the surface.
- $a>>R$: the pattern resembles a sinusoid. This type of pattern passes only once over the surface without any looping movement.

Thus, these three parameters define the shape of the pattern and the number of times which the tool passes over a point on the surface. This number is obtained with Eq. 1.

$$\text{number of passes} = \text{floor}[4 \times R/a + 1] \quad (1)$$

Subsequently, this pattern is applied in a 3D space along the carrier toolpath to impose the number of

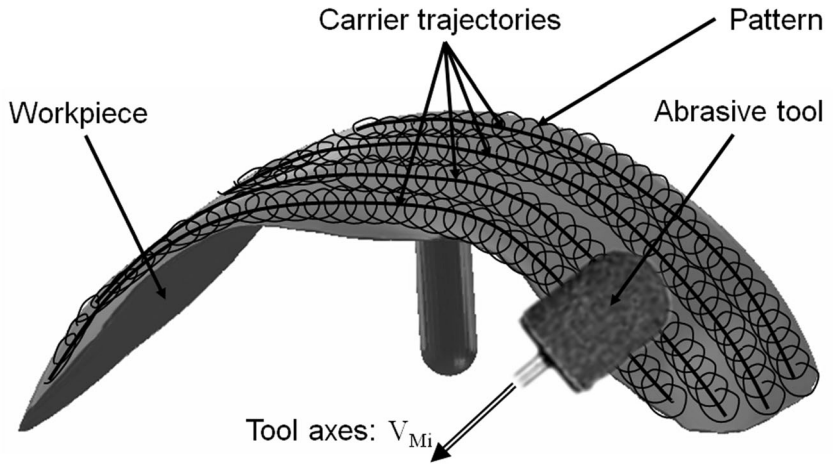

Fig. 3 Example of developed polishing toolpath

patterns per millimeter. Figure 4b illustrates this distortion and presents the parameter N which is the number of patterns per millimeter.

Subsequently, two types of patterns are used: trochoidal and triangular. The first one is the real mathematical trochoidal curve. The second is defined to optimize the surface covering and tool wear. Figure 5 illustrates these two types of patterns.

3 Determination of influential factors using a screening design of experiments

The pre-polishing process proposed has a great number of parameters; see Section 2. These parameters do not all have the same influence on pre-polishing process efficiency and quality. In this section, a DOE is implemented with a screening method to identify the parameters influencing the pre-polishing process cost per volume the most.

3.1 Screening parameters

To carry out the screening test, thresholds and ceilings need to be defined for all factors tested. Table 1 presents these factors with associated parameter names and levels. To carry out this test, a cylindrical ball-end tool is used. This tool has a nominal diameter of 13 mm and a usable cylindrical part of 12 mm. Two types of abrasive caps are used: one with a grit number of 150 and the other with 320. The second factor represents the use of lubricant. The lubricant used is a grinding lubricant with low-fat content and pressure of around 5 bars; 0.05 and 0.1 mm are respectively the threshold and ceiling of the radial engagement tested. RPM values are 6000 and 12,000 rpm, which respectively induce cutting speeds of 245 and 490 m/min. The feed rate values, V_f, are 1000 and 3000 mm/min. The R parameter of the trochoidal pattern is fixed equal to 4 mm. Thereby, 8 mm of the 12.5 mm of the cylindrical part of the tool will be used. Figure 6 illustrates the shape of the pattern used. At the low level (a=40), the pattern resembles a sinusoid and the tool passes only once over the surface. At the high

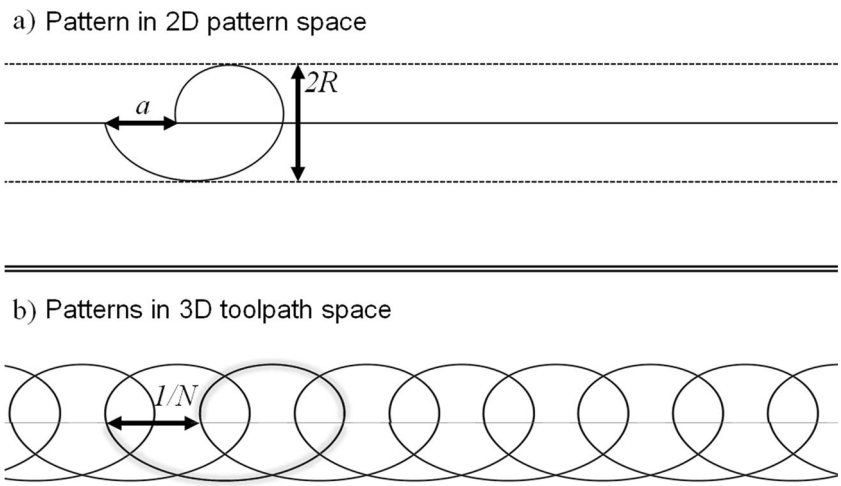

Fig. 4 **a** Definition of the elementary pattern used. **b** Distorted pattern on the carrier toolpath

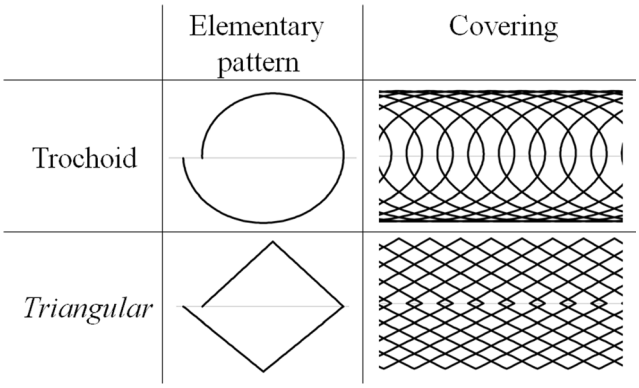

Fig. 5 Two pattern types used

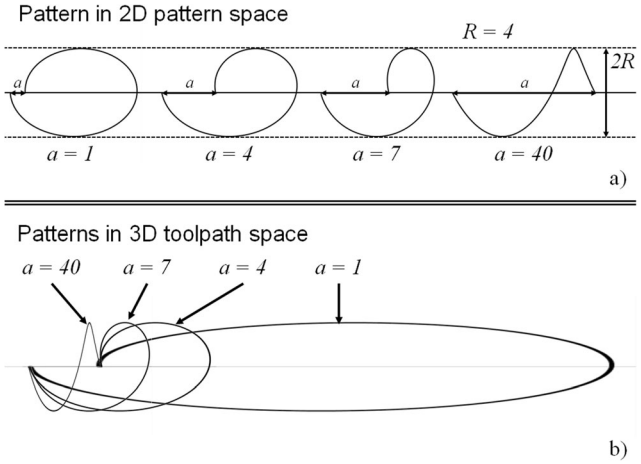

Fig. 6 Pattern shape tested in the DOE

level (a=1), the pattern resembles a circle and the tool passes 17 times over a point on the surface. Two numbers of patterns per millimeter are tested (0.5 and 4 patterns/mm). Moreover, the trochoidal pattern is at threshold level and the optimized, triangular pattern is at ceiling level.

Figure 7 illustrates the experimental environment. The pre-polished surface is a cylinder with 8 mm of diameter in 100Cr6 (steel with 1 % of carbon and 1.5 % of chrome; Brinell hardness 195 HB). Pre-polishing length is 40 mm. Each experiment starts with a fresh surface, and it comprises three passes. Each pass is programmed with the nominal radial engagement. This means that the last pass is programmed with 3 times the radial engagement as compared to the fresh surface.

Table 2 presents the experiment carried out for the screening design of experiment. Twelve experiments are planned with a Hadamard matrix with two repetitions of one test.

3.2 Screening responses: definition of the objective functions

The pre-polishing operation is a semi-finishing operation. Its main objective is to suppress the scallops caused by the rough milling operation (scallops between two ball-end tool passes). Consequently, the objective function was to reduce the pre-polishing cost, maintaining a surface quality to avoid overcost during the finishing step. Equation 2 presents the computation of the pre-polishing cost, PP_cost. This cost is composed of three terms:

- First is the cost of machine time to achieve the pre-polishing operation. This cost is computed with the cost per hour of the machine multiplied by the pre-polishing time. It is the addition of the real pre-polishing time, Time, computed with Eq. 3, and the tool change time. This is equal to the number of tool changes necessary to achieve the pre-polishing operation (N_change computed with Eq. 4) multiplied by the time to change a tool (Time_change).
- Secondly, the cost of the tool (Tool_cost) is deducted using Eq. 6. This equation does not take into account the tool holder cost.

Table 1 Factors tested for the screening design of experiment

Parameter name	Parameter	Threshold (−1)	Ceiling (+1)
$X1$	Grit number	150	320
$X2$	Lubrication	No	Yes
$X3$	Radial engagement (mm)	0.05	0.1
$X4$	RPM (rpm)	6000	12,000
$X5$	V_f (mm/min)	1000	3000
$X6$	a (R=4 mm)	40	1
$X7$	N (patterns/mm)	0.5	4
$X8$	Pattern shape	Trochoidal	Triangular

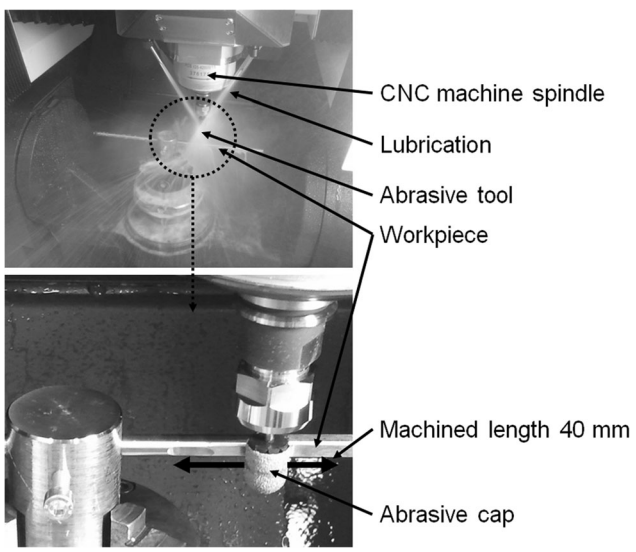

Fig. 7 Pre-polishing tests carried out

Table 2 Experiments carried out with screening design of experiment

Experiment number	Grit number	Lubrication	Radial engagement (mm)	RPM (rpm)	V_f (mm/min)	a	N (patterns/mm)	Pattern
1	320	Yes	0.05	12,000	3000	1	0.5	Trochoidal
2	150	Yes	0.1	6000	3000	1	4	Trochoidal
3	320	No	0.1	12,000	1000	1	4	Triangular
4	150	Yes	0.05	12,000	3000	40	4	Triangular
5	150	No	0.1	6000	3000	1	0.5	Triangular
6	150	No	0.05	12,000	1000	1	4	Trochoidal
7	320	No	0.05	6000	3000	40	4	Triangular
8	320	Yes	0.05	6000	1000	1	0.5	Triangular
9	320	Yes	0.1	6000	1000	40	4	Trochoidal
10	150	Yes	0.1	12,000	1000	40	0.5	Triangular
11	320	No	0.1	12,000	3000	40	0.5	Trochoidal
12	150	No	0.05	6000	1000	40	0.5	Trochoidal
12_1	150	No	0.05	6000	1000	40	0.5	Trochoidal
12_2	150	No	0.05	6000	1000	40	0.5	Trochoidal

– Lastly, the constant cost (Cst) includes, for example, the cost to make the workpiece fixture, preparation cost, etc.

$$\text{PP\_cost} = \text{Time} \times \text{Cost/h} + \text{N\_change} \times \text{Time\_change} \times \text{Cost/h} + \text{Tool\_cost} + \text{Cst} \quad (2)$$

With

Time: the duration of pre-polishing operation, only the time where the tool machines the workpiece
Cost/h: the cost of the 5-axis CNC machine per hour
N_change: the number of tool changes necessary during the pre-polishing operation
Tool_cost: the cost of tools to carry out the pre-polishing operation
Cst: the constant costs in pre-polishing operations.

$$\text{Time} = \text{Vol}/Q \quad (3)$$

With

Vol: the volume of material removal
Q: the material removal flow rate

$$\text{N\_change} = \text{Time}/\text{Tool\_life\_duration} \quad (4)$$

With

Tool_life_duration: the tool life duration computed with Eq. 5. For the computation, this duration is supposed constant for all the tools.

$$\text{Tool\_life\_duration} = \text{Tool\_usable}/\text{Wear\_speed} \quad (5)$$

With

Tool_usable: the usable tool volume
Wear_speed: the wear speed of the usable volume of the tool.

$$\text{Tool\_cost} = \text{N\_change} \times (\text{Caps} + \text{Support}/10) \quad (6)$$

With

Caps: the cost of caps
Support: the support cost; support may be changed about every ten caps.

Equation 7 was obtained by combining Eqs. 2 to 6. This equation highlights that the cost of a pre-polishing operation depends only on material removal flow rate (Q), tool wear speed (Wear_speed), and constant values. Thereafter, the polishing cost will be computed using the following:

– *Material removal flow rate*: this parameter is computed by dividing the material removal by the machining time. Material removal is computed by multiplying the machined length (40 mm, see Fig. 7) by the average machined surface. This surface is obtained by averaging the machined surface at both ends of the machined region. The machined surface, at each end, is computed using the disk portion area equation and measuring the real radial engagement with a micrometer. The machining time is provided by the CNC machine, only the time where the tool machines the workpiece is considered. Q is expressed in cubic millimeters per second.

– *Tool wear speed*: to measure the tool wear, the envelope profile of the tool is measured before and after the pre-polishing operation. This envelope profile is obtained by measuring several tool diameters with a laser CNC machine option. Finally, the wear area between the tool envelope profiles before and after pre-polishing is divided by the machining time to obtain the tool wear speed. Wear_speed is expressed in cubic millimeters per second.

$$\text{PP\_cost} = (\text{Vol}/Q) \times [\text{Cost/h} + \text{Wear\_speed}/\text{Tool\_surface} \times \{\text{Time\_change} \times \text{Cost/h} + (\text{Caps} + \text{Support}/10)\}] + \text{Cst} \quad (7)$$

Furthermore, the machined surface roughness must be controlled. The purpose of the work presented is to optimize the pre-polishing process, but this optimization should not increase the polishing stage time much.

3.3 Screening results and discussions

In the DOE method, screening experiments are used to determine the influential factors. Furthermore, if no interaction is present, screening may also provide information on the direction of influence of each factor on the response parameters. To analyze the screening results, a numerical model (Eq. 8) is associated with the response (Y which represents, firstly, the cost per volume and, secondly, the surface roughness). The best fit is carried out with a Moore–Penrose pseudo-inverse method. In the model obtained, if bi is positive, that means when Xi changes from low to high level, the value of the response increases. Furthermore, the higher the absolute value of bi, the more influence the Xi factor has on the response.

Table 3 provides all the experimental results. The Cost by pre-polished volume is computed using Eq. 7. The numerical values used to carry out this computation are as follows:

Table 3 Experimental results

Experiment number	Q (mm^3/s)	Wear_speed (mm^2/s)	PP_cost/Vol (€/mm^3)	Roughness (μm)
1	0.0156	0.0190	17.35	0.838
2	0.0626	0.0085	2.55	1.57
3	0.0190	0.0028	5.19	0.815
4	0.0244	0.0052	5.12	1.03
5	0.1699	0.0302	2.30	1.77
6	0.0152	0.0020	6.02	1.05
7	0.0097	0.0051	12.64	1.09
8	0.0071	0.0067	19.64	0.896
9	0.0199	0.0024	4.76	0.458
10	0.2339	0.0185	1.14	6.71
11	0.1203	0.0518	5.15	6.02
12	0.0159	0.0196	17.42	3.71
12_1	0.0271	0.0180	9.60	3.53
12_2	0.0244	0.0188	11.07	4.89

– Cost/h is €125/h;
– Caps is €0.5;
– Support is €3.6;
– Time_change is 10 min.

$$Y = b0 + b1{\cdot}X1 + b2{\cdot}X2 + b3{\cdot}X3 + b4{\cdot}X4 + b5{\cdot}X5 + b6{\cdot}X6 + b7{\cdot}X7 + b8{\cdot}X8 \quad (8)$$

With

Xi: the value of the i factor.
bi: the coefficient associated with the i factor.

3.3.1 Pre-polishing cost per volume

The model presented by Eq. 8 is associated with the determined cost per volume (presented in Table 3) to obtain the bi coefficients presented in Table 4. Figure 8 provides the histogram presentation of bi values and the Pareto chart of these values. This curve is obtained by plotting the cumulative effects in percent of each factor starting by the most influential. This curve is used to determine the limit between the factors influencing or not. Below is the classification of factors, starting with the most influential, for reducing production cost per volume:

Table 4 Numerical model of cost by the removed volume

		PP_cost/Vol
	$b0$	8.27
Grit number	$b1$	2.51
Lubrication	$b2$	0.15
Radial engagement	$b3$	−4.76
RPM	$b4$	−1.61
V_f	$b5$	−0.75
a	$b6$	0.57
N	$b7$	−2.23
Pattern	$b8$	−0.60

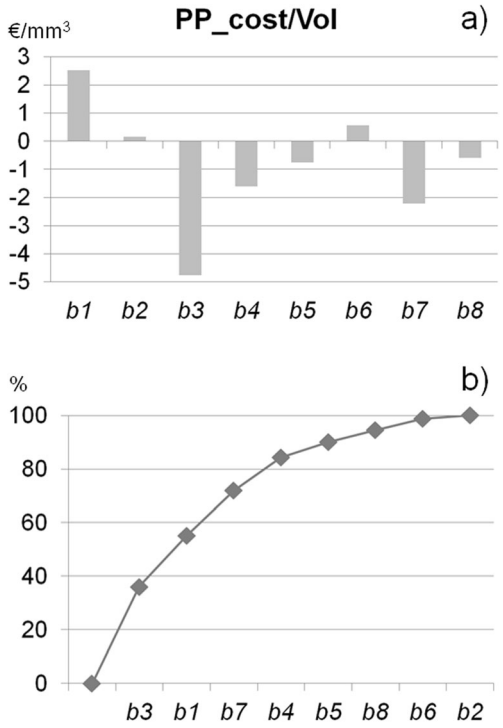

Fig. 8 Model coefficients for pre-polishing cost per volume: **a** histogram and **b** Pareto chart

- *X*3 (very influential): *b*3 value is negative, which means that to reduce the pre-polishing cost, it is necessary to increase the radial engagement.
- *X*1 (influential): a low level of the grit number (150) reduces the production cost. Thereby, a high grit size reduces the operation cost.
- *X*7 (influential): numerous patterns per millimeter are necessary to reduce the pre-polishing cost.
- *X*4 (influential): an augmentation of the spindle rotation decreases the production cost.
- *X*5 (not very influential): to reduce the pre-polishing cost, the feed rate may be increased.
- *X*8 (not very influential): a triangular pattern reduces the production cost compared to a trochoidal pattern.
- *X*6 (not very influential): a pattern that resembles a circle increases the pre-polishing cost compared to a pattern that resembles a sinusoid.
- *X*2 (not influential): lubrication does not significantly influence the pre-polishing cost.

3.3.2 Surface roughness

Surface roughness is an important constraint at the end of the pre-polishing process. Surface roughness measures were accurately characterized through optical measurements using the chromatic confocal sensing coordinate measuring machine (CMM). The resolution of this CMM is about 40 nm. Measurements were carried out on a line of 30 mm with a 4-μm step. Thereafter, the form defect is suppressed and no other filters were added; thereby, the surface undulation is considered in its presented roughness. Next, the arithmetic average is computed without filtering more the form defect suppression. Table 5 and Fig. 9 present the coefficient values of the associated model (Eq. 8). Below is the classification of influential factors, starting with the highest, to reduce surface roughness:

- *X*7 (very influential): increasing the number of patterns per millimeter significantly reduces surface roughness.
- *X*6 (very influential): parameter *a* determines the shape of the pattern and the number of times that the toolpath passes over the same point on the surface (see Section 3.1). With a low value of *X*6, the pattern passes only once over the surface (inducing high roughness), while with the highest value, the pattern passes 17 times.
- *X*3 (influential): an augmentation of the radial engagement induces a degradation of the roughness. This phenomenon may be explained by the augmentation of pre-polishing forces.
- *X*4 (influential): an augmentation of the spindle rotation increases surface roughness.
- *X*1 (influential): a high level of the grit number (320) reduces surface roughness. Thereby, a small grit size reduces roughness.
- *X*2 (not very influential): lubrication improves surface roughness slightly.
- *X*8 (not very influential): a triangular pattern reduces surface roughness slightly compared to a trochoidal pattern.
- *X*5 (not influential): the feed rate does not significantly influence surface roughness.

Table 5 Numerical model of the surface roughness

		Roughness
	*b*0	2.16
Grit number	*b*1	−0.48
Lubrication	*b*2	−0.25
Radial engagement	*b*3	0.73
RPM	*b*4	0.58
V_f	*b*5	−0.11
a	*b*6	−1.01
N	*b*7	−1.16
Pattern	*b*8	−0.11

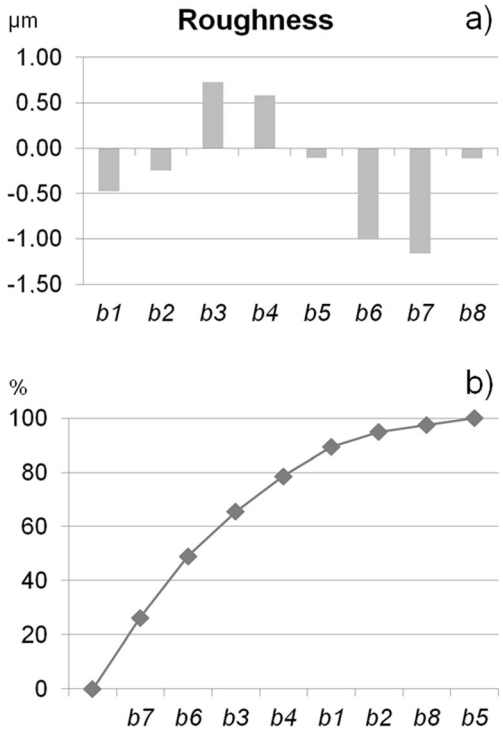

Fig. 9 Model coefficients for surface roughness: **a** histogram and **b** Pareto chart

4 Optimization of factors: response surface of DOE

4.1 Experiment definition

The aim of the proposed work is to optimize the pre-polishing operation factors; this means (Section 3.2) reducing the pre-polishing cost per volume by controlling the surface roughness obtained. The screening design of experiment proposed (Section 3) highlights the influential factors on the pre-polishing operation:

- Pre-polishing cost per volume: three main influential factors are (starting with the highest) $X3$, $X1$, and $X7$.
- Surface roughness is influenced by (starting with the highest) $X7$, $X6$, and $X3$.

The study presented proposes a response surface to optimize three main factors: $X3$, $X6$, and $X7$. These factors will be optimized to reduce pre-polishing cost per volume (objective function defined in Section 3.2) by controlling the surface roughness. On the other hand, other factors are fixed for response surface DOE tests:

- Grit number of 150 ($X1=-1$) to reduce production cost with little effect on surface roughness
- Lubrication off ($X2=-1$): this factor does not have a major influence; the lubrication will be suppressed during the response surface tests.
- RPM ($X4=1$): this factor does not have great effect on pre-polishing optimization and will be selected equal to 12,000 rpm to carry out the response surface tests.
- V_f ($X5=0$): this factor does not have a major influence, and it is fixed at 2000 mm/min for the response surface tests.
- Pattern shape ($X8=1$): using a triangular shape reduces the production cost and improves the surface roughness.

The response surface proposed uses three levels for each factor ($X3$, $X6$, and $X7$). These levels are presented in Table 6. Table 7 presents the experiments carried out and the results obtained. Two response parameters are implemented: pre-polishing cost per volume and surface roughness.

Table 6 Factor values tested in the response surface of DOE

		Low level (−1)	Medium level (0)	High level (+1)
$X3$	Radial engagement (mm)	0.05	0.1	0.15
$X7$	N (patterns/mm)	0.5	2.5	4
$X6$	a (R=4 mm)	7	4	1

Table 7 Response surface experiments and results

Experiment number	$X3$	$X7$	$X6$	Q (mm^3/s)	Wear_speed (mm^2/s)	PP_cost/Vol (€/mm^3)	Roughness (µm)
1	−1	−1	−1	0.0281	0.0182	4.74	2.34
2	1	−1	−1	0.5586	0.0402	0.45	6.74
3	−1	1	−1	0.0099	0.0018	4.50	1.08
4	1	1	−1	0.0987	0.0045	0.60	1.65
5	−1	−1	1	0.0215	0.0171	5.91	2.16
6	1	−1	1	0.3278	0.0216	0.46	1.83
7	−1	1	1	0.0120	0.0023	3.92	1.13
8	1	1	1	0.1964	0.0100	0.45	1.61
9	−1	0	0	0.0157	0.0045	3.75	1.23
10	1	0	0	0.1917	0.0089	0.43	1.32
11	0	−1	0	0.2272	0.0337	0.96	2.45
12	0	1	0	0.1170	0.0108	0.80	1.37
13	0	0	−1	0.0800	0.0064	0.87	1.63
14	0	0	1	0.0669	0.0070	1.09	1.83
15	0	0	0	0.0823	0.0072	0.90	1.71
15_1	0	0	0	0.0998	0.0068	0.72	1.31
15_2	0	0	0	0.0789	0.0074	0.95	1.63
15_3	0	0	0	0.0752	0.0070	0.96	1.75

Table 8 Coefficients of the two response surfaces

	PP_cost/Vol (€/mm^3)	Roughness (μm)
*b*0	0.73	1.42
*b*3	−2.04	0.52
*b*7	−0.23	−0.87
*b*6	0.07	−0.49
*b*33	1.41	−0.07
*b*77	0.19	0.57
*b*66	0.29	0.39
*b*37	0.30	−0.38
*b*36	−0.09	−0.60
*b*76	−0.24	0.64

4.2 Result and discussion

To carry out the optimization step, a model was associated with both responses (cost per volume and roughness). This model is a second-order DOE equation (Eq. 9).

$$Y = b0 + b3{\cdot}X3 + b7 \times X7 + b6 \times X6 + b33{\cdot}X3^2 + b77{\cdot}X7^2 + b66{\cdot}X6^2 + b37{\cdot}X3{\cdot}X7 + b36{\cdot}X3{\cdot}X6 + b76{\cdot}X7{\cdot}X6 \quad (9)$$

Table 8 presents the values of Eq. 9 coefficients for both responses. Subsequently, Table 8 models are presented as a new figure (Figs. 10 and 11). To represent these models (Eq. 9), a 4D space is necessary: 3D for the factors (*X*3, *X*7, and *X*6) and 1D for the response values. To do this, we propose to use a 3D space with one axe for each factor. Thereafter, a sphere is placed along a grid of points on this space. For the figures presented (Figs. 10 and 11), this grid is obtained using the values −1, 0, and 1 on each axis inducing 27 points. The diameter and the color of each sphere are functions of the value of the modeled response in each point. This representation means that the direction of the variation can be easily appreciated.

4.2.1 Cost per pre-polished volume response surface

The objective is to reduce the pre-polishing cost per volume. Figure 4 presents the 4D graph of the modeled cost per pre-polished volume. This figure highlights that low values of radial engagement (*X*3=−1 which corresponds to a radial engagement of 0.05 mm) must be excluded to maintain reasonable production cost. Furthermore, this figure illustrates an optimal value of the production cost close to the points *X*3=1, *X*7=0, and *X*6=0. Mathematically speaking, an optimal value is computed to decrease production cost.

- *X*3=0.72; radial engagement of 0.136 mm
- *X*7=0.04; *N*=2.58 patterns/mm
- *X*6=0.01; *a*=3.96, a pattern which passes 5 times over each point on the toolpath.

4.2.2 Surface roughness

Figure 11 presents the 4D representation of the modeled surface roughness. The result obtained confirms the screening design of experiment (Section 3.3). A low level of *X*7 (few patterns per millimeter) and *X*6 (a pattern which passes a few times over the same point on the surface) combined with a

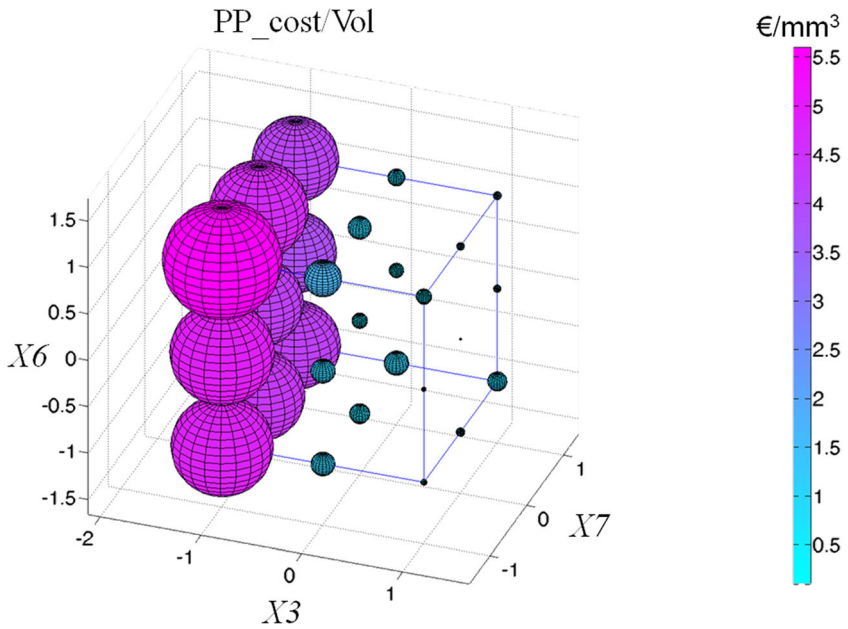

Fig. 10 Response surface of the cost by the removed volume

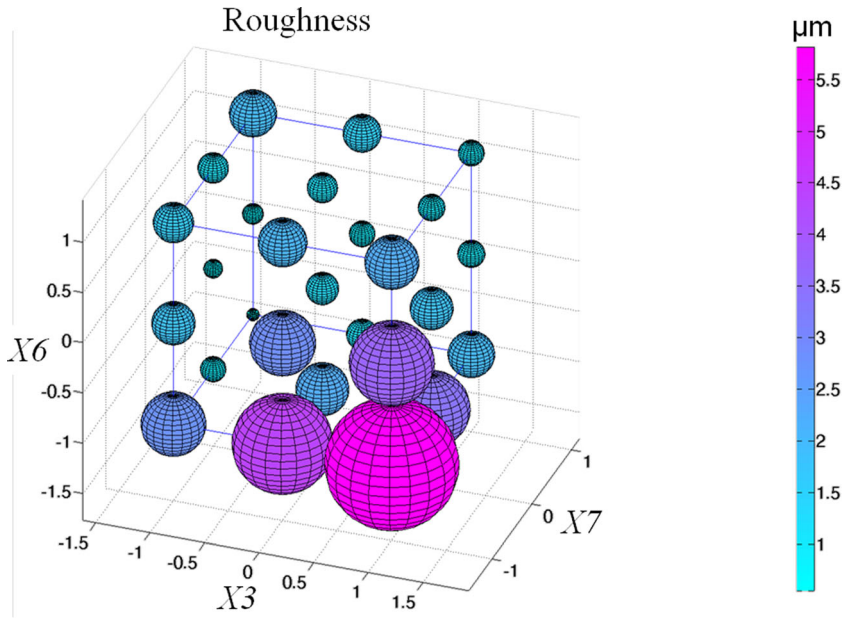

Fig. 11 Response surface of the roughness

high level of *X*3 (high radial engagement) results in the poor roughness of the tested area. With this model, the optimized point seen in Section 4.2.1 provides a roughness value of 1.7 µm.

4.2.3 Constrained optimization

A constrained optimization is carried out to find the cheapest pre-polishing parameters to ensure a specified roughness. Indeed, using a numerical solver and the obtained model of cost and roughness (presented respectively in Sections 4.2.1 and 4.2.2), the optimal values of the *X*3, *X*6, and *X*7 factors are determined to reduce the pre-polishing cost, ensuring the specified roughness. Table 9 presents the optimal pre-polishing parameters to reduce the cost, ensuring the specified roughness.

Results of Table 9 are plotted on Fig. 12. This figure highlights two main areas:

– The value of the roughness specified is between 1.1 and 1.8 µm. Section 3.3 demonstrates that the radial engagement (*X*3) plays the major role in pre-polishing cost. Thus, in this first area, the optimal value of *X*3

Table 9 Optimal pre-polishing parameters used to reduce the cost by ensuring the specified roughness

Specified roughness (µm)	*X*3	*X*7	*X*6	PP_cost/Vol (€/mm^3)
1.8	0.7220	0.0384	0.0125	0.33
1.7	0.7218	0.0403	0.0138	0.33
1.6	0.7152	0.1011	0.0544	0.33
1.5	0.7081	0.1683	0.0996	0.33
1.4	0.7003	0.2445	0.1514	0.33
1.3	0.6917	0.3346	0.2138	0.34
1.2	0.6827	0.4511	0.2982	0.35
1.1	0.0730	0.7350	0.0920	0.40
1	−0.2698	0.7742	−0.1803	1.63
0.9	−0.4848	0.7989	−0.3487	2.28
0.8	−0.6558	0.8177	−0.4811	2.90
0.7	−0.8020	0.8352	−0.5955	3.50
0.6	−0.9319	0.8495	−0.6964	4.09
0.55	−0.9922	0.8568	−0.7435	4.38

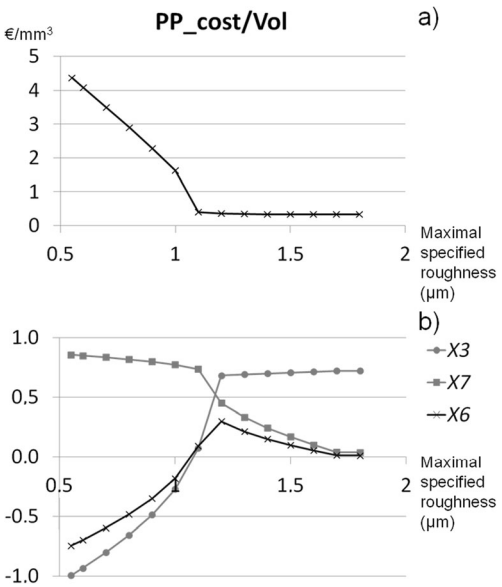

Fig. 12 Optimal pre-polishing parameters used to reduce the cost by ensuring the specified roughness

is constant and only the number of patterns per millimeter ($X7$) and the pattern shape ($X6$, which define number of times that the tool passes over a point on the surface) increase.
– The value of roughness specified is between 0.55 and 1 μm. With the specified roughness of less than 1 μm, it is impossible to maintain the radial engagement, inducing a great increase in pre-polishing cost.

5 Conclusions

This paper proposes a method to carry out pre-polishing and polishing operations on a common 5-axis milling machine. The method proposed uses a flexible tool comprising sandpaper caps mounted on a rubber support. The pre-polishing operation is carried out with a toolpath composed of a carrier trajectory on which an elementary optimized pattern is repeated. The study presented proposes an optimization of this process using a design of experiment. The aim of the optimization is to reduce the pre-polishing process cost by controlling the roughness.

The screening design of experiment implemented highlights that to carry out this aim, big grit sizes with a triangular pattern type need to be used. These experiments also highlight that the lubrication, RPM, and feed rate do not play a major role in pre-polishing cost. Furthermore, three main factors must be compromised to optimize the pre-polishing process: radial engagement, number of patterns per millimeter, and pattern shape. These factors are optimized using a response surface. This method provides empirical models to estimate the pre-polishing material removal flow rate, the tool wear speed response surface, the cost per pre-polished volume response surface, and resulting roughness. Finally, these models are used to define the optimal factors. This optimization highlights two areas based on imposed surface roughness. The first one, which accepts large surface roughness (between 1.1 and 1.8 μm), authorizes a large radial engagement (0.136 mm) with reduced pre-polishing cost. On the other hand, in the second area (roughness$<$1 μm), the radial engagement must be reduced, thus inducing significant increase in production cost.

Acknowledgments The experimental devices were founded by the European Community, French Ministry of Research and Education, Pays d'Aix Conurbation Community and Aix-Marseille University.

References

1. Hilerio I, Mathia T, Alepee C (2004) 3D measurements of the knee prosthesis surfaces applied in optimizing of manufacturing process. Wear 257:1230–1234. doi:10.1016/j.wear.2004.05.027
2. Lison D, Lauwerys R, Demedts M, Nemery B (1996) Experimental research into the pathogenesis of cobalt/hard metal lung disease. Eur Respir J 9:1024–1028. doi:10.1183/09031936.96.09051024
3. Tsai MJ, Huang JF (2006) Efficient automatic polishing process with a new compliant abrasive tool. Int J Adv Manuf Technol 30: 817–827. doi:10.1007/s00170-005-0126-6
4. Roswell A, Xi F, Liu G (2006) Modelling and analysis of contact stress for automated polishing. Int J Mach Tools Manuf 46:424–435. doi:10.1016/j.ijmachtools.2005.05.006
5. Liao L, Xi F, Liu K (2008) Modeling and control of automated polishing/deburring process using a dual-purpose compliant toolhead. Int J Mach Tools Manuf 48:1454–1463. doi:10.1016/j.ijmachtools.2008.04.009
6. Ryuh BS, Park SM, Pennock GR (2006) An automatic tool changer and integrated software for a robotic die polishing station. Mech Mach Theory 41:415–432. doi:10.1016/j.mechmachtheory.2005.06.004
7. Nagata F, Hase T, Haga Z, Omoto M, Watanabe K (2007) CAD/CAM-based position/force controller for a mold polishing robot. Mechatronics 17:207–216. doi:10.1016/j.mechatronics.2007.01.003
8. Lin FY, Lu TS (2005) Development of a robot system for complex surfaces polishing based on CL data. Int J Adv Manuf Technol 26: 1132–1137. doi:10.1007/s00170-004-2088-5
9. Wu X, Kita Y, Ikoku K (2007) New polishing technology of free form surface by GC. J Mater Process Technol 187:81–84. doi:10.1016/j.jmatprotec.2006.11.218
10. Pessoles X, Tournier C (2009) Automatic polishing process of plastic injection molds on a 5-axis milling center. J Mater Process Technol 209:3665–3673. doi:10.1016/j.jmatprotec.2008.08.034
11. Feng D, Sun Y, Du H (2014) Investigations on the automatic precision polishing of curved surfaces using a five-axis machining centre. Int J Adv Manuf Technol 72:1625–1637. doi:10.1007/s00170-014-5774-y
12. Chaves-Jacob J, Linares JM, Sprauel JM (2013) Improving tool wear and surface covering in polishing via toolpath optimization. J Mater Process Technol 213:1661–1668. doi:10.1016/j.jmatprotec.2013.04.005
13. Wang G, Wang Y, Xu Z (2009) Modeling and analysis of the material removal depth for stone polishing. J Mater Process Technol 209:2453–2463. doi:10.1016/j.jmatprotec.2008.05.041
14. Ahn JH, Lee MC, Jeong HD, Kim SR, Cho KK (2002) Intelligently automated polishing for high quality surface formation of sculptured die. J Mater Process Technol 130:339–344. doi:10.1016/S0924-0136(02)00821-X
15. Denkena B, De Leon L, Turger A, Behrens L (2010) Prediction of contact conditions and theoretical roughness in manufacturing of complex implants by toric grinding tools. Int J Mach Tools Manuf 50:630–636. doi:10.1016/j.ijmachtools.2010.03.008
16. Savio G, Meneghello R, Concheri G (2009) A surface roughness predictive model in deterministic polishing of ground glass moulds. Int J Mach Tools Manuf 49:1–7. doi:10.1016/j.ijmachtools.2008.09.001
17. Xi F, Zhou D (2005) Modeling surface roughness in the stone polishing process. Int J Mach Tools Manuf 45:365–372. doi:10.1016/j.ijmachtools.2004.09.016
18. Huissoon JP, Ismail F, Jafari A, Bedi S (2002) Automated polishing of die steel surfaces. Int J Adv Manuf Technol 19:285–290. doi:10.1007/s001700200036
19. Chaves-Jacob J, Linares JM, Sprauel JM (2015) Control of the contact force in a pre-polishing operation of free-form surfaces realised with a 5-axis CNC machine. CIRP Ann Manuf Technol 64:309–312. doi:10.1016/j.cirp.2015.04.008